

## Interaction of Formamide with the Ru(001) Surface

J. E. Parmeter,<sup>†</sup> U. Schwalke,<sup>‡</sup> and W. H. Weinberg\**Contribution from the Division of Chemistry and Chemical Engineering, California Institute of Technology, Pasadena, California 91125. Received March 16, 1987*

**Abstract:** The adsorption and decomposition of formamide (NH<sub>2</sub>CHO) on the hexagonally close-packed Ru(001) surface have been studied by using high-resolution electron energy loss spectroscopy and thermal desorption mass spectrometry. At 80 K, the initial adsorption of formamide results in CH bond cleavage and the formation of an  $\eta^2(\text{C,O})\text{-NH}_2\text{CO}$  species. This species decomposes upon annealing to 250 K, leaving a mixture of CO, NH<sub>3</sub>, NH, and hydrogen adatoms on the surface. The NH<sub>3</sub> and CO desorb near 315 and 480 K, respectively, whereas the NH decomposes below 400 K to nitrogen and hydrogen adatoms. Recombinative desorption of H<sub>2</sub> occurs at 420 K, while recombinative desorption of N<sub>2</sub> occurs near 770 K. For higher initial formamide coverages (where the fractional coverage of formamide that decomposes exceeds approximately 0.05 monolayer), molecular adsorption in an  $\eta^1(\text{O})\text{-NH}_2\text{CHO}$  configuration is observed also at 80 K. This species undergoes competing desorption and decomposition at 225 K to an intermediate believed to be N-bonded NHCHO, which in turn converts to a species tentatively identified as  $\eta^1(\text{N})\text{-NCHO}$  at 300 K. The latter species decomposes to chemisorbed CO, N, and H near 375 K. Following a saturation formamide exposure on Ru(001) at 80 K, approximately 0.15 monolayer of formamide decomposes upon subsequent annealing, with approximately two-thirds of the total decomposing via the  $\eta^2(\text{C,O})\text{-NH}_2\text{CO}$  intermediate and the remainder reacting via the  $\eta^1(\text{O})\text{-NH}_2\text{CHO}$ .

## I. Introduction

High-resolution electron energy loss spectroscopy (EELS) has emerged as one of the most important experimental techniques for studying the reactions of molecules on well-characterized metal surfaces,<sup>1</sup> especially in delimiting reaction mechanisms via the isolation of reaction intermediates. Such studies are of interest not only because of the obvious importance of understanding molecule-metal surface interactions in heterogeneous catalytic processes but also because they allow comparisons to be made between the bonding and reactivity of various ligands in multi-nuclear homogeneous metal clusters and that on metal surfaces. Recently, we have reported the results of an EELS and thermal desorption mass spectrometric (TDMS) study of the interaction of formamide (NH<sub>2</sub>CHO) with the Ru(001)-p(1×2)-O surface, i.e., the hexagonally close-packed ruthenium surface on which an ordered p(1×2) overlayer of oxygen adatoms (fractional coverage of one-half) is present.<sup>2</sup> We report here the results of an EELS and TDMS study of the adsorption and decomposition of formamide on the clean (reduced) Ru(001) surface.

From the point of view of chemisorption, formamide is a rather complex molecule, containing two heteroatoms and a carbonyl double bond. Thus, there are several ways that formamide might adsorb molecularly on a metal surface: via the electron lone pairs on the oxygen and/or nitrogen atoms (although in gas-phase formamide there is no electron lone pair isolated strictly on the nitrogen atom), or in an  $\eta^2(\text{C,O})$  configuration with rehybridization of the carbonyl double bond. A number of decomposition intermediates are also possible, as may be appreciated by considering the variety of formamide-derived ligands that have been identified in organometallic compounds. These include  $\eta^1(\text{C})\text{-CONHR}$ ,<sup>3</sup>  $\eta^1(\text{N})\text{-NHCOR}$ ,<sup>4</sup>  $\eta^2(\text{C,O})\text{-NR}_2\text{CO}$ ,<sup>5</sup>  $\eta^2(\text{N,O})\text{-NRCHO}$  (both chelating and bridging),<sup>6</sup> and the tautomers  $\eta^2(\text{C,N})\text{-HOCNR}$  and  $\eta^2(\text{C,N})\text{-OCNHR}$  (R = H, alkyl, or aryl).<sup>7</sup> These species are depicted schematically in Figure 1 with R = H, the case relevant to formamide decomposition on a metal surface.

In our study of formamide chemisorption on the Ru(001)-p(1×2)-O surface,<sup>2</sup> it was found that below 225 K formamide bonds to the surface via a lone pair of electrons on the oxygen atom, i.e., the formamide adsorbs molecularly below 225 K in an  $\eta^1(\text{O})\text{-NH}_2\text{CHO}$  configuration. At 225 K, the  $\eta^1(\text{O})\text{-NH}_2\text{CHO}$  converts to  $\eta^2(\text{N,O})\text{-NH}_2\text{CHO}$  that is bonded to the surface via electron lone pairs on both the oxygen and nitrogen atoms. The  $\eta^2(\text{N,O})\text{-NH}_2\text{CHO}$  converts near 260 K to  $\eta^2(\text{N,O})\text{-NHCHO}$ ,

the nitrogen-containing analogue of the  $\eta^2$ -formate that has been identified previously on Ru(001) as an intermediate in the decomposition of formic acid.<sup>8</sup> For sufficiently high initial formamide coverages, both of these conversions are accompanied by some molecular desorption of formamide. The  $\eta^2(\text{N,O})\text{-NHCHO}$  is stable on the Ru(001)-p(1×2)-O surface to 420 K, at which temperature it decomposes, evolving gaseous CO and H<sub>2</sub> and leaving nitrogen adatoms on the surface. The nitrogen adatoms recombine and desorb as N<sub>2</sub> near 570 K, leaving the p(1×2)-O overlayer intact. For a saturation formamide exposure, approximately 0.05 monolayer of  $\eta^2(\text{N,O})\text{-NHCHO}$  is formed and decomposes on this surface. (A monolayer is defined as  $1.58 \times 10^{15}$  cm<sup>-2</sup>, the density of ruthenium atoms on the Ru(001) surface.)

Electronegative adsorbates such as oxygen adatoms can alter the chemical reactivity of metal surfaces, just as electron-withdrawing ligands modify the properties and reactivity of organometallic compounds. Comparing the reactions of formamide on the Ru(001)-p(1×2)-O surface and on clean Ru(001) is of particular interest in view of the fact that ordered oxygen over-

(1) Ibach, H.; Mills, D. L. *Electron Energy Loss Spectroscopy and Surface Vibrations*; Academic: New York, 1982.

(2) (a) Parmeter, J. E.; Schwalke, U.; Weinberg, W. H. *J. Am. Chem. Soc.* **1987**, *109*, 1876. (b) Parmeter, J. E.; Schwalke, U.; Weinberg, W. H. *J. Am. Chem. Soc.* **1987**, *109*, 5083.

(3) (a) Kruse, A. E.; Angelici, R. J. *J. Organomet. Chem.* **1970**, *24*, 231. (b) Behrens, H.; Jungbauer, A. Z. *Naturforsch.* **1979**, *34b*, 1477. (c) Sacco, A.; Giannoccaro, P.; Vasapollo, G. *Inorg. Chim. Acta* **1984**, *83*, 125. (d) Lindsay, A. J.; Kim, S.; Jacobson, R. A.; Angelici, R. J. *Organometallics* **1984**, *3*, 1523.

(4) Burgess, K.; Johnson, B. F. G.; Lewis, J. J. *Chem. Soc., Dalton Trans.* **1983**, 1179.

(5) (a) Fagan, P. J.; Manriquez, J. M.; Vollmer, S. H.; Day, C. S.; Day, V. W.; Marks, T. J. *J. Am. Chem. Soc.* **1981**, *103*, 2206. (b) Azam, K. A.; Yin, C. C.; Deeming, A. J. *J. Chem. Soc., Dalton Trans.* **1978**, 1201. (c) Szostak, R.; Strouse, C. E.; Kaesz, H. D. *J. Organomet. Chem.* **1980**, *191*, 243. (d) Mayr, A.; Lin, Y.-C.; Boag, N. M.; Kaesz, H. D. *Inorg. Chem.* **1982**, *21*, 1704. (e) Kampe, C. E.; Boag, N. M.; Kaesz, H. D. *J. Mol. Catal.* **1983**, *21*, 297.

(6) (a) Rossi, R.; Duatti, A.; Magon, L.; Casellato, U.; Graziani, R.; Toniolo, L. *Inorg. Chim. Acta* **1983**, *74*, 77. (b) Sahajpal, A.; Robinson, R. D. *Inorg. Chem.* **1979**, *18*, 3572. (c) Schwering, H.-U.; Weidlein, J. *Chimia* **1973**, *27*, 535. (d) Jennings, J. R.; Wade, K.; Wyatt, B. K. *J. Chem. Soc. A* **1968**, 2535. (e) Adams, R. D.; Golembeski, N. M. *J. Organomet. Chem.* **1979**, *171*, C21. (f) Adams, R. D.; Golembeski, N. M.; Selegue, J. P. *Inorg. Chem.* **1981**, *20*, 1242.

(7) (a) Lin, Y. C.; Knobler, C. B.; Kaesz, H. D. *J. Am. Chem. Soc.* **1981**, *103*, 1216. (b) Kaesz, H. D.; Knobler, C. B.; Andrews, M. A.; van Buskirk, G.; Szostak, R.; Strouse, C. E.; Lin, Y. C.; Mayr, A. *Pure Appl. Chem.* **1982**, *54*, 131.

(8) (a) Avery, N. R.; Toby, B. H.; Anton, A. B.; Weinberg, W. H. *Surf. Sci.* **1982**, *122*, L574. (b) Toby, B. H.; Avery, N. R.; Anton, A. B.; Weinberg, W. H. *J. Electron Spectrosc. Relat. Phenom.* **1983**, *29*, 317.

<sup>†</sup> AT&T Bell Laboratories Predoctoral Fellow.

<sup>‡</sup> Feodor-Lynen Research Fellow of the Alexander von Humboldt Foundation.

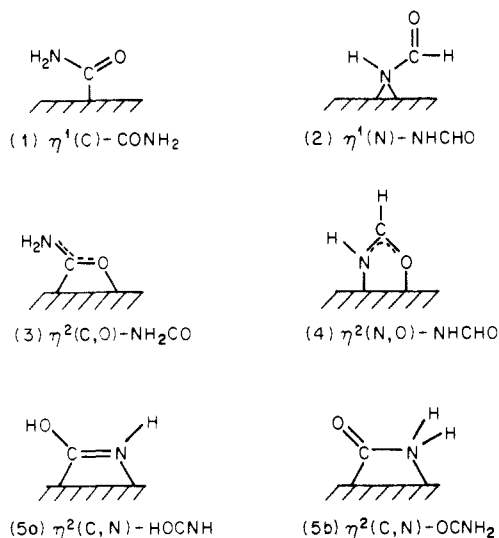


**Figure 1.** Several possible decomposition products of formamide on a metal surface. All of these species have known organometallic analogues (in some of which one or both hydrogens are replaced by an alkyl or aryl group).

layers are known to alter the chemistry of both acetone<sup>9</sup> and formaldehyde<sup>10</sup> on Ru(001). On clean Ru(001), both acetone and formaldehyde adsorb at 80 K principally via rehybridization of the CO double bond in an  $\eta^2(\text{C},\text{O})$  configuration. In the case of formaldehyde, some decomposition to CO,  $\eta^2(\text{C},\text{O})-\text{HCO}$ , and hydrogen adatoms occurs as well. On the Ru(001)-p(2 $\times$ 2)-O surface, adsorption at 80 K of both molecules occurs primarily in an  $\eta^1(\text{O})$  configuration, with bonding to the surface occurring via an electron lone pair on the oxygen atom. Thus, in the case of the adsorption of formamide on clean Ru(001) at 80 K, we might expect the formation of  $\eta^2(\text{C},\text{O})-\text{NH}_2\text{CHO}$  or  $\eta^2(\text{C},\text{O})-\text{NH}_2\text{CO}$ , rather than the formation of  $\eta^1(\text{O})-\text{NH}_2\text{CHO}$ , which occurs on the Ru(001)-p(1 $\times$ 2)-O surface. Such species could also lead to different decomposition products compared to those from  $\eta^1(\text{O})-\text{NH}_2\text{CHO}$ .

## II. Experimental Details

The EEL spectrometer and the ultrahigh vacuum (UHV) chamber housing it have been described elsewhere,<sup>11</sup> as have the methods of cleaning the Ru(001) crystal<sup>12</sup> and handling the formamide.<sup>2</sup> Typical parameters for the EEL spectra shown and discussed in this paper are the following: resolution (full-width at half-maximum of the elastically scattered electron beam), 70–80 cm<sup>-1</sup>; count rate (elastically scattered peak),  $2 \times 10^5$  Hz; impact energy of the incident electron beam, 4 eV; and (fixed) angle of incidence of the electron beam, 60° with respect to the surface normal. All EEL spectra were measured in the specular direction, except when it is stated explicitly otherwise. The UHV chamber also contained a quadrupole mass spectrometer for performing TDMS measurements and for an analysis of background gases. The heating rate in all thermal desorption spectra was approximately 8 K·s<sup>-1</sup>. The base pressure in the UHV chamber was less than 10<sup>-10</sup> Torr. Liquid nitrogen cooling allowed crystal temperatures as low as 80 K to be attained. The crystal was heated resistively and cleaned by annealing in a background of oxygen or, occasionally, by argon ion sputtering.

The NH<sub>2</sub>CHO used in this study was obtained from Aldrich with a reported purity of 99% and was purified further as discussed elsewhere.<sup>2</sup> Its purity was verified in situ with mass spectrometry. Both EELS and TDMS experiments were also performed with N-deuteriated formamide, ND<sub>2</sub>CHO (MSD Isotopes, 98 at % D). Although H/D exchange into

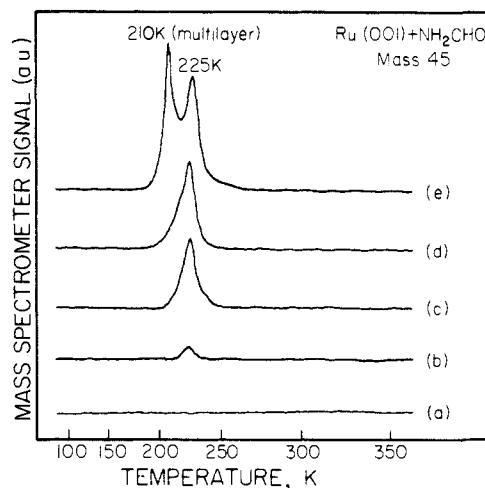


**Figure 2.** The molecular formamide ( $m/e = 45$  amu) thermal desorption spectra that result following various exposures of NH<sub>2</sub>CHO to the clean Ru(001) surface at 80 K. The approximate formamide exposures are (a) 2 L, (b) 4 L, (c) 6 L, (d) 8 L, and (e) 12 L.

the ND<sub>2</sub> group resulted in the presence of small amounts of NHDCHO and/or NH<sub>2</sub>CHO in the ND<sub>2</sub>CHO,<sup>13</sup> these experiments were nevertheless useful in helping to assign various EELS loss features, and they also yielded qualitative information concerning H<sub>2</sub> thermal desorption.

## III. Results

**A. Thermal Desorption Mass Spectrometry.** Following a saturation exposure of formamide on the clean Ru(001) surface at 80 K, five different species are observed to desorb between approximately 200 and 800 K, namely, molecular formamide, carbon monoxide, hydrogen, nitrogen, and ammonia.<sup>14</sup> Species specifically looked for and not observed to desorb include H<sub>2</sub>O, HCN, NO, and H<sub>2</sub>CO. The five molecular species detected with TDMS are discussed separately below.

**1. Molecular Formamide.** Figure 2 shows a series of thermal desorption spectra of NH<sub>2</sub>CHO ( $m/e = 45$  amu) following various exposures of formamide to the clean Ru(001) surface at 80 K. For exposures less than approximately 4 L (1 L = 1 Langmuir  $\approx 10^{-6}$  Torr·s), no molecular desorption occurs, indicating that at low coverages all of the adsorbed formamide decomposes. For exposures greater than approximately 4 L, a molecular desorption peak appears at 225 K. The peak temperature does not shift with increasing exposures (i.e., coverage), indicative of a first-order desorption reaction. Assuming a preexponential factor of the desorption rate coefficient of 10<sup>13</sup> s<sup>-1</sup>, an activation energy of desorption (equal to the heat of adsorption since adsorption is not activated) of approximately 13 kcal·mol<sup>-1</sup> is calculated for this desorption state.<sup>15</sup> This desorption feature is most likely due to monolayer rather than second layer formamide,<sup>2</sup> especially since the amount of formamide that decomposes (approximately 0.15 monolayer, cf. Section III.A.2) seems very low to correspond to monolayer saturation. For exposures greater than approximately 8 L, a second thermal desorption peak appears at 210 K. This peak does not saturate with increasing exposure and is due to the desorption of condensed formamide multilayers, in agreement with previous results for formamide desorption from the Ru(001)-p(1 $\times$ 2)-O surface.<sup>2</sup>

(13) The exchange of hydrogen into the ND<sub>2</sub> group of ND<sub>2</sub>CHO may occur in the metal line through which formamide is passed before entering the UHV chamber or on the walls of the UHV chamber.

(14) Since the amount of ammonia desorbed is very small, it was difficult to detect via TDMS in the EELS chamber, and these TDMS experiments were carried out in a companion UHV chamber in which the mass spectrometer is closer to the crystal. The production of ammonia was also demonstrated unambiguously by EELS. For previous TDMS results concerning ammonia on Ru(001), see: (a) Benndorf, C.; Madey, T. E. *Surf. Sci.* **1983**, *135*, 164. (b) Danielson, L.; Dresser, M. J.; Donaldson, E. E.; Dickinson, J. T. *Surf. Sci.* **1978**, *71*, 599. In ref 14a, the saturation (monolayer) coverage of ammonia on Ru(001) was estimated to be 0.25 monolayer.

(15) Redhead, P. A. *Vacuum* **1962**, 203.

(9) (a) Avery, N. R.; Anton, A. B.; Toby, B. H.; Weinberg, W. H. *J. Electron Spectrosc. Relat. Phenom.* **1983**, *29*, 233. (b) Avery, N. R.; Weinberg, W. H.; Anton, A. B.; Toby, B. H. *Phys. Rev. Lett.* **1983**, *51*, 682. (c) Anton, A. B.; Parmeter, J. E.; Weinberg, W. H. *J. Am. Chem. Soc.* **1986**, *108*, 684.

(10) (a) Anton, A. B.; Parmeter, J. E.; Weinberg, W. H. *J. Am. Chem. Soc.* **1985**, *107*, 5558. (b) Anton, A. B.; Parmeter, J. E.; Weinberg, W. H. *J. Am. Chem. Soc.* **1985**, *108*, 1823.

(11) Thomas, G. E.; Weinberg, W. H. *Rev. Sci. Instrum.* **1979**, *50*, 497.

(12) Thomas, G. E.; Weinberg, W. H. *J. Chem. Phys.* **1979**, *70*, 954.

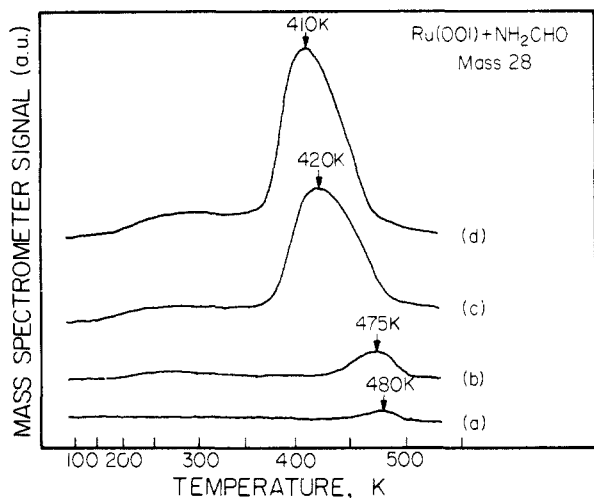


**Figure 3.** Thermal desorption spectra of CO ( $m/e = 28$  amu) that result following various exposures of  $\text{NH}_2\text{CHO}$  to the clean Ru(001) surface at 80 K. The approximate formamide exposures are (a) 0.3 L, (b) 1 L, (c) 5 L, and (d) 10 L.

**2. Carbon Monoxide.** Thermal desorption spectra of CO ( $m/e = 28$  amu) following various exposures of  $\text{NH}_2\text{CHO}$  to Ru(001) at 80 K are shown in Figure 3. There is a single CO thermal desorption peak that occurs at 480 K for the lowest exposures studied (fractional surface coverage of CO desorbed of approximately 0.01 monolayer) and shifts downward to 410 K at saturation. Despite this downshift in peak temperature with increasing coverage, this is a first-order, desorption-limited reaction, since low coverages of chemisorbed CO on clean Ru(001) also desorb near 480 K,<sup>16</sup> the recombinative desorption of CO formed from carbon and oxygen adatoms occurs only above 500 K on this surface,<sup>17</sup> and EEL spectra show clearly that molecularly adsorbed CO is present from 250 to above 400 K (cf. Section III.B). The most reasonable cause of the downshift in the CO desorption temperature with increasing formamide exposures is the increasing coverage of nitrogen adatoms between 400 and 500 K, which are also present due to formamide decomposition (cf. Section III.B). The ruthenium-carbon bond of adsorbed CO is formed by electron donation from the  $5\sigma$  (carbon lone pair) orbital of CO to the surface, accompanied by electron back-donation from the metal  $sd$ -band to the  $2\pi^*$  antibonding orbital of CO.<sup>18</sup> The (relatively) electronegative nitrogen adatoms withdraw electron density from the surface ruthenium atoms, presumably reducing the extent of the back-bonding and leading to a lowered CO desorption temperature. A similar effect has been observed for CO that is coadsorbed with ordered overlayers of oxygen adatoms on Ru(001).<sup>19</sup>

The saturation coverage of CO on Ru(001) is known to be approximately 0.68 monolayer.<sup>20</sup> Since all of the formamide that decomposes on the Ru(001) surface gives rise to CO as a reaction product, there is a one-to-one correspondence between the amount of CO that desorbs for a given formamide coverage and the amount of formamide that decomposes. Thus, by comparing the time-integrated intensities of the CO thermal desorption peaks for saturation exposures of both CO and  $\text{NH}_2\text{CHO}$ , the amount of  $\text{NH}_2\text{CHO}$  that decomposes for a saturation formamide exposure may be calculated. This comparison yields an estimate of 0.15

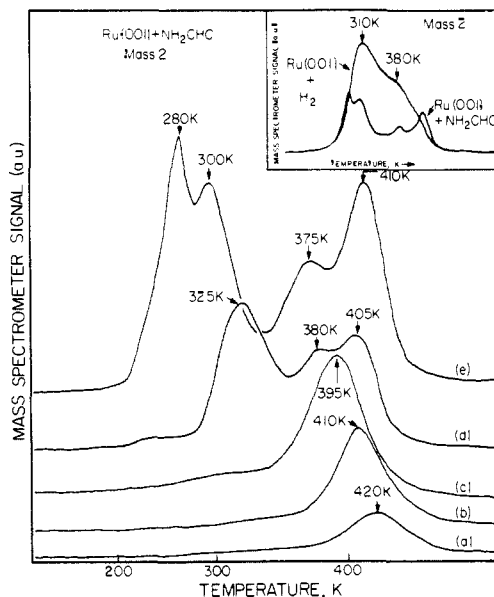


**Figure 4.** Thermal desorption spectra of  $\text{H}_2$  ( $m/e = 2$  amu) that result following various exposures of  $\text{NH}_2\text{CHO}$  to the clean Ru(001) surface at 80 K. The inset compares  $\text{H}_2$  thermal desorption spectra that result following saturation exposures of  $\text{H}_2$  and  $\text{NH}_2\text{CHO}$  on this surface. The approximate formamide exposures are (a) 0.5 L, (b) 1 L, (c) 2 L, (d) 4 L, and (e) 10 L.

monolayer of irreversibly adsorbed  $\text{NH}_2\text{CHO}$  following a saturation formamide exposure on Ru(001) at 80 K, or approximately  $2.3 \times 10^{14}$  molecules- $\text{cm}^{-2}$ .

**3. Hydrogen.** Figure 4 shows a series of  $\text{H}_2$  ( $m/e = 2$  amu) thermal desorption spectra that were measured following various  $\text{NH}_2\text{CHO}$  exposures to Ru(001) at 80 K, as well as the  $\text{H}_2$  thermal desorption spectrum that results following a saturation exposure of  $\text{H}_2$  on Ru(001). For an exposure of 0.5 L of formamide there is a single desorption peak at 420 K, which shifts downward with increasing exposures. This is a second-order desorption peak resulting from the recombinative desorption of hydrogen adatoms, since the  $\text{H}_2$  thermal desorption spectra that result from 0.5–1-L formamide exposures are nearly identical with those that result from low  $\text{H}_2$  exposures on Ru(001), where the adsorption is dissociative and the desorption is second-order.<sup>21</sup> For a 2-L  $\text{NH}_2\text{CHO}$  exposure, the single  $\text{H}_2$  desorption peak has downshifted to 395 K. Following a 4-L exposure, three peaks appear at 325, 380, and 405 K. Finally, a 10-L exposure (slightly greater than saturation) gives rise to a rather complex desorption spectrum, with the three previously mentioned peaks now at 300, 375, and 410 K and a fourth peak at 280 K.

Thermal desorption spectra of  $\text{H}_2$ , HD, and  $\text{D}_2$  following saturation exposures of  $\text{ND}_2\text{CHO}$  on Ru(001) (not shown) were also measured in order to determine the origin of the hydrogen desorbing in the four peaks of Figure 4e. The 410 K peak consisted almost entirely of  $\text{D}_2$  with a small amount of HD, indicating that the hydrogen desorbing in this peak originates primarily, if not entirely, from the  $\text{NH}_2$  group of the formamide. (It should be recalled that a small amount of  $\text{NHDCHO}$  and/or  $\text{NH}_2\text{CHO}$  was present in the  $\text{ND}_2\text{CHO}$  sample.) The peak at 375 K was very rich in HD and contained no  $\text{D}_2$ . Sample contamination precluded a quantitative analysis of the relative amounts of  $\text{H}_2$ , HD, and  $\text{D}_2$  desorbing in each peak.

Since the saturation coverage of hydrogen adatoms on Ru(001) is known to be approximately 0.85,<sup>21</sup> and the amount of  $\text{NH}_2\text{CHO}$  that decomposes following a saturation exposure on Ru(001) is known to be approximately 0.15 from the CO thermal desorption data discussed above, the  $\text{H}_2$  thermal desorption spectra may be

(16) (a) Madey, T. E.; Menzel, D. *J. Appl. Phys.* **1974**, *Suppl. 2*, Pt. 2, 229. (b) Pfnür, H.; Feulner, P.; Engelhardt, H. A.; Menzel, D. *Chem. Phys. Lett.* **1978**, *59*, 481. (c) Pfnür, H.; Feulner, P.; Menzel, D. *J. Chem. Phys.* **1983**, *79*, 4613.

(17) Hills, M. M.; Parmeter, J. E.; Weinberg, W. H. *J. Am. Chem. Soc.*, submitted for publication.

(18) (a) Blyholder, G. *J. Phys. Chem.* **1964**, *68*, 2772. (b) Blyholder, G. *J. Phys. Chem.* **1975**, *79*, 756.

(19) Anton, A. B.; Avery, N. R.; Madey, T. E.; Weinberg, W. H. *J. Chem. Phys.* **1986**, *85*, 507.

(20) Pfnür, H.; Menzel, D.; Hoffmann, F. M.; Ortega, A.; Bradshaw, A. M. *Surf. Sci.* **1980**, *93*, 431.

(21) (a) Shimizu, H.; Christmann, K.; Ertl, G. *J. Catal.* **1980**, *61*, 412. (b) Schwarz, J. A. *Surf. Sci.* **1979**, *87*, 525. (c) Barteau, M. A.; Broughton, J. Q.; Menzel, D. *Surf. Sci.* **1983**, *88*, 384. (d) Conrad, H.; Scala, R.; Stenzel, W.; Unwin, R. *J. Chem. Phys.* **1984**, *81*, 6371.

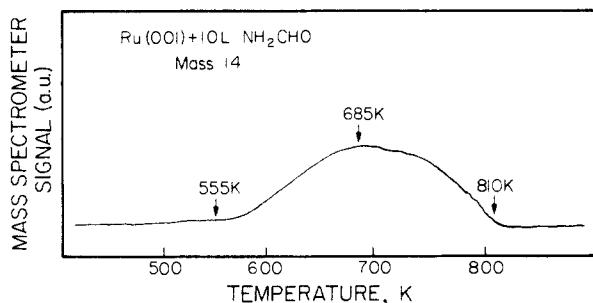


**Figure 5.** The  $m/e = 14$  amu (N cracking fragment of  $N_2$ ) thermal desorption spectrum that results following a saturation exposure of  $NH_2CHO$  to the clean Ru(001) surface at 80 K.

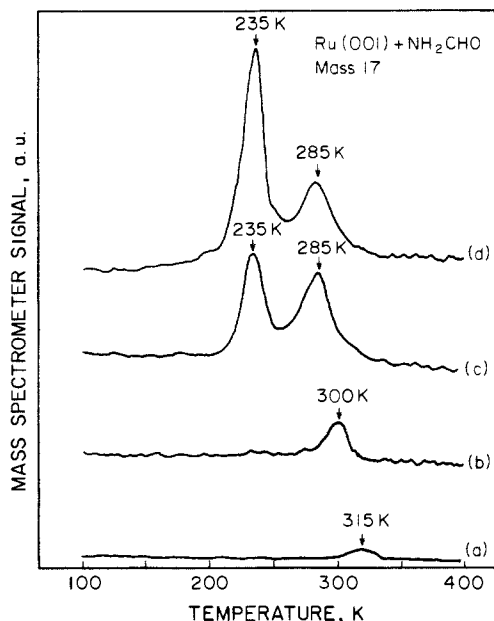


**Figure 6.** Thermal desorption spectra for  $m/e = 17$  amu that result when the Ru(001) surface at 80 K is exposed to approximately (a) 0.4 L, (b) 2 L, (c) 5 L, and (d) 8 L of formamide. Only the high-temperature feature corresponds to ammonia desorption; the peak at 235 K is due to a molecular formamide cracking fragment.

used to estimate very approximately the amount of  $NH_3$  that is formed and desorbed following a saturation formamide exposure. The hydrogen thermal desorption spectra indicate that approximately 0.39 monolayer of hydrogen adatoms are desorbed as  $H_2$ , corresponding to the decomposition of 0.13 monolayer of  $NH_2CHO$ . The amount of ammonia that is desorbed is thus approximately  $0.15 - 0.13 = 0.02$  monolayer. Although the absolute accuracy of this estimate is poor (probably no better than a factor of 2), it is clear that the amounts of  $H_2$  and CO that desorb are in a ratio of nearly 3:2, so that most of the formamide that decomposes must produce only CO,  $H_2$ , and  $N_2$  as desorption products. The amount of  $NH_3$  that is desorbed is quite small, and the formation of  $NH_3$  represents a minor reaction pathway.

**4. Nitrogen.** Figure 5 shows the  $m/e = 14$  amu (N cracking fragment of  $N_2$ , which distinguishes it from CO) thermal desorption spectrum that results following a saturation exposure of  $NH_2CHO$  on Ru(001) at 80 K. Nitrogen is desorbed between approximately 555 and 810 K, with a maximum desorption rate near 685 K. For a 0.5-L  $NH_2CHO$  exposure, the nitrogen desorbs with a peak temperature of approximately 770 K. The fact that molecularly adsorbed  $N_2$  on Ru(001) desorbs below 150 K<sup>22</sup> and the clear evidence for the presence of nitrogen adatoms in EEL spectra measured following  $NH_2CHO$  adsorption and annealing to above 400 K (cf. Section III.B) prove unambiguously that this desorption of  $N_2$  results from the recombinative desorption of

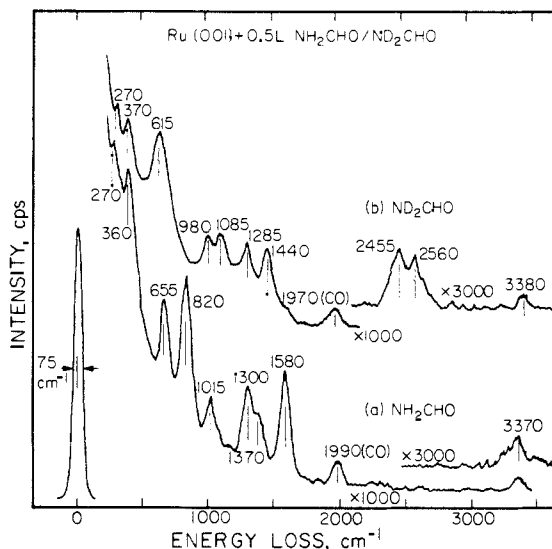


**Figure 7.** The EEL spectra that result following 0.5-L exposures of (a)  $NH_2CHO$  and (b)  $ND_2CHO$  to the clean Ru(001) surface at 80 K. These spectra are characteristic of  $\eta^2(C,O)-NH_2CO$  and  $\eta^2(C,O)-ND_2CO$ .

nitrogen adatoms that are formed from the decomposition of formamide.

**5. Ammonia.** Thermal desorption spectra for  $m/e = 17$  amu following various exposures of formamide to the Ru(001) surface at 80 K are shown in Figure 6. Thermal desorption spectra of mass 18 were also measured, and the lack of water desorption verifies that the desorption peaks in Figure 6 do not correspond to an OH cracking fragment of desorbed  $H_2O$ . However, the 235 K thermal desorption peak appears at the same temperature and coverage as a molecular formamide thermal desorption peak and appears to be due entirely to a formamide cracking fragment. Thus, only the desorption peak at 285–315 K is due to ammonia desorption. Ammonia desorption is observed for all formamide exposures, which ranged from 0.3 L to saturation. At low coverage, the peak temperature is 315 K, and it shifts down in temperature to 285 K when this peak is saturated. Since ammonia is identified clearly with EELS (cf. Figure 8) this ammonia desorption peak appears to be mainly desorption-limited. The initial desorption temperature of 315 K is in agreement with the results of a previous, detailed study of ammonia adsorption on clean Ru(001), in which it was shown that ammonia desorbed in a single peak centered at 315 K for initial ammonia coverages less than approximately 15% of saturation.<sup>14</sup> The total amount of ammonia that desorbs following a saturation formamide exposure is estimated to be  $\leq 0.02$  monolayer, based on the previously discussed CO and  $H_2$  thermal desorption measurements. Essentially all of the ammonia that is formed desorbs rather than decomposes.<sup>14</sup>

**B. Electron Energy Loss Spectroscopy.** In discussing the EEL spectra of  $NH_2CHO$  on Ru(001), it is convenient to consider separately two distinct coverage regimes. For low initial coverages (exposures  $< 2$  L, where the amount of  $NH_2CHO$  that decomposes is less than approximately 0.05 monolayer), only a single surface species is detected by EELS following adsorption at 80 K. For higher coverages (exposures  $> 2$  L, where the amount of formamide decomposing is greater than approximately 0.05 monolayer), an additional surface species is present at 80 K due to the passivation of the surface by the products of the initial adsorption reaction. The low and high coverage regimes are thus treated separately below.

**1. Low Coverage.** The EEL spectra that result following 0.5-L exposures of  $NH_2CHO$  and  $ND_2CHO$  to the clean Ru(001) surface at 80 K are shown in Figure 7. In both spectra there is a weak loss feature near 2000  $cm^{-1}$  due to  $\nu(CO)$  of a very small amount ( $< 0.005$  monolayer) of coadsorbed CO. This CO is adsorbed from the chamber background and is not due to formamide decomposition. In addition, the  $ND_2CHO$  spectrum shows a weak  $\nu(NH)$  loss feature at 3380  $cm^{-1}$  due to a small amount

(22) See ref 19 above, as well as: Anton, A. B.; Avery, N. R.; Toby, B. H.; Weinberg, W. H. *J. Electron Spectrosc. Relat. Phenom.* **1983**, *29*, 181.

of NHDCHO and/or NH<sub>2</sub>CHO contamination. The other loss features in both spectra disappear concomitantly upon annealing to approximately 250 K and may therefore be assigned to a single surface species that is formed upon the adsorption of formamide at 80 K.

For a number of reasons, the species present on the surface at 80 K may be identified as NH<sub>2</sub>CO. First, both spectra of Figure 7 show no evidence of a carbon-hydrogen stretching mode in the 2800–3100-cm<sup>-1</sup> region, and corresponding spectra measured off-specular also show no evidence of a  $\nu$ (CH) mode. The latter measurement is of importance because  $\nu$ (CH) modes are often detected most easily in off-specular EEL spectra.<sup>1</sup> Since the  $\nu$ (CH) mode is clearly detected in several formamide-derived species (including the parent molecule) on the Ru(001)-p(1×2)-O surface,<sup>2</sup> it is concluded that carbon-hydrogen bond cleavage has occurred upon the adsorption of formamide at 80 K. Second, since there are no vibrational modes in either spectrum due to oxygen adatoms,<sup>23</sup> nitrogen adatoms (see Figure 9c), or CO (other than a trivial amount of CO adsorbed from the chamber background), it is apparent that the carbon-nitrogen and carbon-oxygen bonds of formamide remain intact. This conclusion is justified since our previous studies of formamide decomposition on Ru(001)-p(1×2)-O show that loss features due to carbon monoxide and atomic oxygen are easily detected in the presence of coadsorbed formamide and its decomposition products.<sup>2</sup> Third, the clear presence of two nitrogen-deuterium stretching modes in the ND<sub>2</sub>CHO spectrum, the NH<sub>2</sub> wagging mode at 820 cm<sup>-1</sup> which shifts down to approximately 600 cm<sup>-1</sup> upon N-deuteration and the mode at 1580 cm<sup>-1</sup> in the NH<sub>2</sub>CHO spectrum which shifts down markedly upon N-deuteration [indicating that this mode has substantial  $\delta$ (NH<sub>2</sub>) character], all indicate that the NH<sub>2</sub> bonds are not broken. Taken together, these arguments serve to identify the species that is present on the surface as NH<sub>2</sub>CO. Such a species may be either  $\eta^1$ (C)-bonded,<sup>3</sup>  $\eta^2$ (C,O)-bonded,<sup>5</sup> or  $\eta^2$ (C,N)-bonded<sup>7</sup> (cf. Figure 1, illustrations 1, 3, and 5b). However,  $\eta^2$ (C,N)-OCNH<sub>2</sub> species in organometallic compounds exhibit strong  $\nu$ (CO) modes near 1775 cm<sup>-1</sup>,<sup>7</sup> and all organometallic analogues of  $\eta^1$ (C)-CONH<sub>2</sub> exhibit strong  $\nu$ (CO) stretching modes between 1500 and 1650 cm<sup>-1</sup>.<sup>3</sup> Since these modes are clearly lacking in Figure 7b, the surface species is identified as  $\eta^2$ (C,O)-NH<sub>2</sub>CO. Since the carbon-oxygen bond of the  $\eta^2$ (C,O)-NH<sub>2</sub>CO has undergone substantial rehybridization, its bond order is significantly less than two. The precise carbon-oxygen and carbon-nitrogen bond orders are somewhat indeterminate, however, since several resonance structures may be drawn for this surface species (cf. Section IV). It might be noted in passing that the observation of two metal-ligand stretching frequencies (see below) is another argument that the surface species present is not  $\eta^1$ (C)-CONH<sub>2</sub>.<sup>24</sup> It should be pointed out that hydrogen adatoms are also present on the surface together with the  $\eta^2$ (C,O)-NH<sub>2</sub>CO, but they are not detected by EELS due to their very weak loss features.

Due to substantial coupling among several vibrational modes of  $\eta^2$ (C,O)-NH<sub>2</sub>CO and  $\eta^2$ (C,O)-ND<sub>2</sub>CO, a complete mode assignment is not possible without the benefit of a normal mode analysis. However, several of the observed loss features may be assigned unambiguously. The peaks at 270 (270) and 360 (370) cm<sup>-1</sup> in the case of  $\eta^2$ (C,O)-NH<sub>2</sub>CO ( $\eta^2$ (C,O)-ND<sub>2</sub>CO) are both assigned to ruthenium-NH<sub>2</sub>CO stretching modes. The peak at 820 cm<sup>-1</sup> in Figure 7a shifts down to approximately 600 cm<sup>-1</sup> upon N-deuteration, so that it overlaps with the peak at 655 cm<sup>-1</sup>, forming a single broad feature centered at 615 cm<sup>-1</sup>. As stated above, the 820-cm<sup>-1</sup> peak is thus identified as the NH<sub>2</sub> wagging mode,  $\omega$ (NH<sub>2</sub>), and the peak at 655 cm<sup>-1</sup> is identified as the NCO bending mode,  $\delta$ (NCO). The peak at 3370 cm<sup>-1</sup> in Figure 7a is due to the unresolved  $\nu_s$ (NH<sub>2</sub>) and  $\nu_a$ (NH<sub>2</sub>) modes, while in the case of  $\eta^2$ (C,O)-ND<sub>2</sub>CO,  $\nu_s$ (ND<sub>2</sub>) and  $\nu_a$ (ND<sub>2</sub>) occur at 2455 and

**Table I.** Frequencies (cm<sup>-1</sup>) of the Observed Vibrational Modes of  $\eta^2$ (C,O)-NH<sub>2</sub>CO and  $\eta^2$ (C,O)-ND<sub>2</sub>CO on Ru(001)

mode	$\eta^2$ (C,O)-NH <sub>2</sub> CO	$\eta^2$ (C,O)-ND <sub>2</sub> CO	freq shift
$\nu_a$ (NH <sub>2</sub> )	3370 <sup>b</sup>	2560	~1.32
$\nu_s$ (NH <sub>2</sub> )		2455	~1.37
see text <sup>a</sup>	1580, 1370	1440, 1285	
	1300, 1015	1085, 980	
$\omega$ (NH <sub>2</sub> )	820	~600 <sup>c</sup>	~1.37
$\delta$ (NCO)	655	~650 <sup>c</sup>	~1.01
$\nu$ (Ru-NH <sub>2</sub> CO)	360	370	0.97
	270	270	1.00

<sup>a</sup> Coupling among these four modes precludes specific mode assignments. The (uncoupled) modes involved are  $\nu_s$ (NCO),  $\nu_a$ (NCO),  $\delta$ -(NH<sub>2</sub>), and  $\rho$ (NH<sub>2</sub>). <sup>b</sup> This feature is broad, and the  $\nu_a$ (NH<sub>2</sub>) and  $\nu_s$ -(NH<sub>2</sub>) modes are not resolved clearly. <sup>c</sup> These two modes overlap in the case of  $\eta^2$ (C,O)-ND<sub>2</sub>CO.

**Table II.** Frequencies (cm<sup>-1</sup>) and Mode Assignments for Liquid NH<sub>2</sub>CHO, Liquid ND<sub>2</sub>CHO, and Gas-Phase NH<sub>2</sub>CHO<sup>a</sup>

mode	NH <sub>2</sub> CHO(l) <sup>43</sup>	ND <sub>2</sub> CHO(l) <sup>43</sup>	NH <sub>2</sub> CHO(g) <sup>44</sup>
$\nu_a$ (NH <sub>2</sub> )	3330	2556	3545
$\nu_s$ (NH <sub>2</sub> )	3190	2385	3451
$\nu$ (CH)	2882	2887	2852
$\nu$ (CO)	1690	1667	1734
$\delta$ (NH <sub>2</sub> )	1608	1118	1572
$\delta$ (CH)	1391	1398	1378
$\nu$ (CN)	1309	1338	1255
$\pi$ (CH)	1056	1056	1030
$\rho$ (NH <sub>2</sub> )	1090	912	1059
$\omega$ (NH <sub>2</sub> )	750	450	602
$\tau$ (NH <sub>2</sub> )	200		289
$\delta$ (NCO)	608	570	565

<sup>a</sup> a = asymmetric, s = symmetric.

2560 cm<sup>-1</sup>, respectively. Four additional peaks appear in each spectrum, at 1015, 1300, 1370, and 1580 cm<sup>-1</sup> for  $\eta^2$ (C,O)-NH<sub>2</sub>CO and at 980, 1085, 1285, and 1440 cm<sup>-1</sup> for  $\eta^2$ (C,O)-ND<sub>2</sub>CO. In the case of  $\eta^2$ (C,O)-NH<sub>2</sub>CO, four modes are expected between 1000 and 1600 cm<sup>-1</sup>, as observed: the symmetric and asymmetric NCO stretching modes, and the NH<sub>2</sub> scissoring and rocking modes. However, coupling among these four modes is evidently significant and renders the mode descriptions  $\nu_s$ (NCO),  $\nu_a$ (NCO),  $\delta$ (NH<sub>2</sub>), and  $\rho$ (NH<sub>2</sub>) rather meaningless. We note again, however, that the 1580-cm<sup>-1</sup> mode in Figure 7a must have substantial  $\delta$ (NH<sub>2</sub>) character, since the highest of these four "middle frequency modes" of  $\eta^2$ (C,O)-ND<sub>2</sub>CO occurs at a frequency 140 cm<sup>-1</sup> lower than this. The observed vibrational frequencies and partial mode assignments for  $\eta^2$ (C,O)-NH<sub>2</sub>CO and  $\eta^2$ (C,O)-ND<sub>2</sub>CO are summarized in Table I. For comparison, Table II provides vibrational frequencies and mode assignments for liquid and gas-phase formamide.

The EEL spectra of low coverages of formamide adsorbed on clean Ru(001) at 80 K show that  $\eta^2$ (C,O)-NH<sub>2</sub>CO remains on the surface when the surface is annealed briefly to temperatures below approximately 230 K, at which point decomposition of the  $\eta^2$ (C,O)-NH<sub>2</sub>CO begins. The only change in the EEL spectra for annealing temperatures below 230 K is that following annealing to 200 K the  $\omega$ (NH<sub>2</sub>) mode [ $\omega$ (ND<sub>2</sub>) in the case of  $\eta^2$ (C,O)-ND<sub>2</sub>CO] increases in intensity by approximately a factor of 2, while the intensities of the other vibrational modes of  $\eta^2$ (C,O)-NH<sub>2</sub>CO remain essentially constant. This suggests a reorientation of the NH<sub>2</sub> group as the surface is heated. The intensity of the  $\omega$ (NH<sub>2</sub>) mode is expected to be greatest when it involves motion of the NH<sub>2</sub> hydrogen atoms that is largely perpendicular to the surface.<sup>25</sup>

Annealing the Ru(001) surface on which low coverages of  $\eta^2$ (C,O)-NH<sub>2</sub>CO are present to 250 K causes the vibrational features due to  $\eta^2$ (C,O)-NH<sub>2</sub>CO to disappear completely, leaving the EEL spectrum shown in Figure 8a. This EEL spectrum is

(23) Thomas, G. E.; Weinberg, W. H. *J. Chem. Phys.* **1978**, *69*, 3611.

(24) An additional argument against  $\eta^1$ (C)-NH<sub>2</sub>CO is the fact that this ligand is known in organometallic chemistry only in compounds containing a single metal atom. When more than one metal atom is present, the observed bonding configuration is  $\eta^2$ (C,O)-NH<sub>2</sub>CO or, more rarely,  $\eta^2$ (C,N)-OCNH<sub>2</sub>. See ref 3, 5, and 7.

(25) This is a consequence of the so-called surface dipole selection rule. See Chapters 1 and 3 of ref 1.

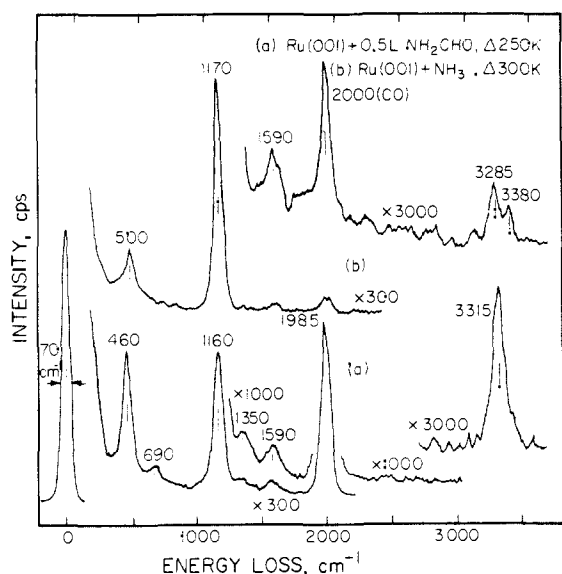


**Figure 8.** (a) The EEL spectrum that results when the Ru(001) surface represented in Figure 7a is annealed briefly to 250 K. (b) The EEL spectrum that results when the clean Ru(001) surface at 80 K is exposed to approximately 1 L of  $\text{NH}_3$  and annealed to 300 K.

**Table III.** Summary of Vibrational Frequencies ( $\text{cm}^{-1}$ ) and Mode Assignments for the Decomposition Products of  $\eta^2(\text{C,O})\text{-NH}_2\text{CO}$  on Ru(001) after Annealing to 250–300 K

species	mode	freq	species	mode	freq
CO	$\nu(\text{CO})$	1985	NH	$\nu(\text{NH})$	3315
	$\nu(\text{Ru-CO})$	460		$\delta(\text{NH})$	1350
NH <sub>3</sub>	$\nu(\text{NH}_3)^a$	3315	$\nu(\text{Ru-NH})$	690	
	$\delta_a(\text{NH}_3)$	1590			
	$\nu_s(\text{NH}_3)$	1160			

<sup>a</sup> The  $\nu_s(\text{NH}_3)$  and  $\nu_a(\text{NH}_3)$  modes of adsorbed  $\text{NH}_3$  are not resolved from the  $\nu(\text{NH})$  mode of coadsorbed NH.

characterized by intense peaks at 460, 1160, and 1985  $\text{cm}^{-1}$  and by weak peaks at approximately 690, 1350, 1590, and 3315  $\text{cm}^{-1}$ . The intense peaks at 460 and 1985  $\text{cm}^{-1}$  are identified easily as  $\nu(\text{Ru-C})$  and  $\nu(\text{CO})$  of carbon monoxide adsorbed in on-top sites.<sup>20,26</sup> On the basis of a comparison to an EEL spectrum of ammonia adsorbed on the Ru(001) surface at 80 K and annealed briefly to 300 K ( $\theta_{\text{NH}_3} \sim 0.02\text{--}0.03$  monolayer) (Figure 8b), the peaks at 1160, 1590, and (in part) 3315  $\text{cm}^{-1}$  are identified as being due to adsorbed ammonia. Previous EELS studies of  $\text{NH}_3$  adsorbed on Pt(111),<sup>27</sup> Ag(110),<sup>28</sup> Ni(111),<sup>29</sup> Ni(110),<sup>29</sup> and Fe(110)<sup>30</sup> have yielded very similar EEL spectra, and these modes are assigned as  $\delta_s(\text{NH}_3)$ ,  $\delta_a(\text{NH}_3)$ , and  $\nu(\text{NH}_3)$ , respectively. Finally, the modes at 690 and 1350  $\text{cm}^{-1}$ , and part of the intensity of the 3315- $\text{cm}^{-1}$  mode, are due to a third surface species that is identified as adsorbed NH. The mode assignments for this species are the following:  $\nu(\text{NH})$ , 3315  $\text{cm}^{-1}$ ;  $\delta(\text{NH})$ , 1350  $\text{cm}^{-1}$ ; and  $\nu(\text{Ru-NH})$ , 690  $\text{cm}^{-1}$  (see below). Thus the three spectroscopically isolated decomposition products of  $\eta^2(\text{C,O})\text{-NH}_2\text{CO}$  on Ru(001) are CO,  $\text{NH}_3$ , and NH.<sup>31</sup> The mode assignments of the EEL spectrum of Figure 8a are summarized in Table III.

When the Ru(001) surface on which  $\eta^2(\text{C,O})\text{-ND}_2\text{CO}$  is adsorbed is annealed to 250 K, the CO modes are again observed at 460 and 1985  $\text{cm}^{-1}$ . Rather than a single sharp and intense peak at 1160  $\text{cm}^{-1}$ , however, four overlapping peaks are observed between 900 and 1160  $\text{cm}^{-1}$  due to the symmetric deformation mode of four different ammonia isotopes:  $\text{ND}_3$ ,  $\text{ND}_2\text{H}$ ,  $\text{NDH}_2$ ,

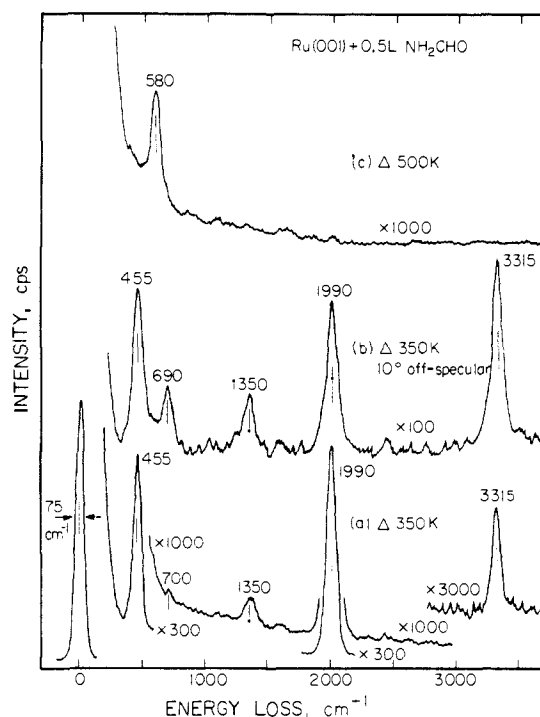


**Figure 9.** (a) The EEL spectrum that results when the Ru(001) surface represented in Figure 7a is annealed briefly to 350 K. (b) An EEL spectrum of the same surface measured  $10^\circ$  off-specular. (c) The EEL spectrum that results when the surface represented in Figure 7a is annealed briefly to 500 K.

and  $\text{NH}_3$ . The observed frequencies are 900  $\text{cm}^{-1}$  ( $\text{ND}_3$ ), 990  $\text{cm}^{-1}$  ( $\text{ND}_2\text{H}$ ), 1090  $\text{cm}^{-1}$  ( $\text{NDH}_2$ ), and 1160  $\text{cm}^{-1}$  ( $\text{NH}_3$ ). The major species formed is  $\text{ND}_2\text{H}$ , and substantial amounts of  $\text{ND}_3$  are also formed. (A crude estimate based on the intensities of the symmetric deformation modes is that the ratio of  $\text{ND}_2\text{H}$  to  $\text{ND}_3$  is approximately 3:2). A  $\nu(\text{ND})$  loss feature is present at 2450  $\text{cm}^{-1}$ , and a weak  $\nu(\text{NH})$  loss feature is present at 3295  $\text{cm}^{-1}$ . The  $\nu_a$  modes of the various ammonia isotopes, as well as the  $\nu(\text{ND})$  mode of coadsorbed ND, are not well resolved. However, an ND species is undoubtedly present and contributes to the intensity of the  $\nu(\text{ND})$  loss feature.

Annealing the surface represented by Figure 8a to 350 K causes the adsorbed ammonia to desorb molecularly, leaving only CO and NH in subsequent EEL spectra<sup>31</sup> and allowing a more definitive characterization of the NH species. Figure 9a shows the specular EEL spectrum of the surface following annealing to 350 K, while Figure 9b shows the EEL spectrum of the same surface, but measured  $10^\circ$  off-specular toward the surface normal. The importance of the off-specular spectrum is that it allows the weak  $\nu(\text{Ru-NH})$  mode of adsorbed NH at 690  $\text{cm}^{-1}$  to be resolved much more clearly from the tail of the elastic peak that is attenuated more rapidly than the loss peaks in off-specular measurements. Note that annealing from 250 K (Figure 8a) to 350 K (Figure 9a) causes the integrated intensity of the  $\nu(\text{NH})$  mode at 3315  $\text{cm}^{-1}$  to decrease by only approximately 40%, indicating that the NH does indeed contribute significantly to the intensity of this mode in Figure 8a. Table IV lists the vibrational modes of adsorbed NH and compares them to those of the adsorbed NH species identified previously as a product of hydrazine decomposition on Ni(111).<sup>32</sup> The observed  $\delta(\text{NH})$  frequency of 1350  $\text{cm}^{-1}$  is well within the range of 1200–1420  $\text{cm}^{-1}$  observed for  $\delta(\text{NH})$  in organic imides.<sup>33</sup> Table IV also lists the vibrational

(26) (a) Thomas, G. E.; Weinberg, W. H. *J. Chem. Phys.* **1979**, *70*, 1437. (b) References 12 and 20.

(27) Sexton, B. A.; Mitchell, G. E. *Surf. Sci.* **1980**, *99*, 523.

(28) Gland, J. L.; Sexton, B. A.; Mitchell, G. E. *Surf. Sci.* **1982**, *115*, 623.

(29) Fisher, G. B.; Mitchell, G. E. *J. Electron Spectrosc. Relat. Phenom.* **1983**, *29*, 253.

(30) Erley, W.; Ibach, H. *Surf. Sci.* **1982**, *119*, L357.

(31) Hydrogen adatoms are also present on the surface but are not detected by EELS due to their small cross section for inelastic scattering.<sup>21d</sup>

(32) Glant, J. L.; Fisher, G. B.; Mitchell, G. E. *Chem. Phys. Lett.* **1985**, *119*, 89.

(33) (a) Bigotto, A.; Galasso, V. *Spectrochim. Acta* **1979**, *35A*, 725. (b) Woldbaek, T.; Klæboe, P.; Christensen, D. H. *Acta Chem. Scand.* **1976**, *A30*, 531.

frequencies of the various modes of ND formed from ND<sub>2</sub>CHO decomposition on Ru(001), which are the following:  $\nu(\text{ND})$ , 2460 cm<sup>-1</sup>;  $\delta(\text{ND})$ , 1050 cm<sup>-1</sup>; and  $\nu(\text{Ru-ND})$ , 680 cm<sup>-1</sup>. The corresponding vibrational frequencies of ND on Ni(111) are listed as well.

Annealing the Ru(001) surface to just over 400 K results in the decomposition of NH, leaving only CO, nitrogen adatoms, and a small amount of hydrogen adatoms on the surface. The nitrogen adatoms are identified by a loss feature at 580 cm<sup>-1</sup> due to the vibration of these atoms perpendicular to the surface, i.e.,  $\nu_s(\text{RuN})$ . This mode appears as a shoulder on the  $\nu_s(\text{RuC})$  mode of coadsorbed carbon monoxide, when the latter is present. Annealing to 500 K desorbs the CO (and all remaining hydrogen), leaving only nitrogen adatoms on the surface (Figure 9c). The  $\nu_s(\text{RuN})$  mode of the nitrogen adatoms remains present (and of nearly constant intensity) in EEL spectra after the surface is annealed to 700 K and then attenuates and disappears as the surface is annealed to just over 800 K, in agreement with the N<sub>2</sub> thermal desorption results for low coverages of formamide.

**2. High Coverage.** For initial formamide exposures at 80 K that are greater than approximately 2 L (but below the exposures necessary to condense formamide multilayers), both  $\eta^2(\text{C,O})\text{-NH}_2\text{CO}$  and molecular formamide are observed as adsorption products with EELS. The molecular formamide is  $\eta^1(\text{O})\text{-NH}_2\text{CHO}$ , the same species that is formed following formamide adsorption at 80 K on the Ru(001)-p(1×2)-O surface.<sup>2</sup> Although many of the loss features due to  $\eta^1(\text{O})\text{-NH}_2\text{CHO}$  overlap to some degree the loss features due to  $\eta^2(\text{C,O})\text{-NH}_2\text{CO}$ , the  $\nu(\text{CO})$  loss peak of the former species is quite strong and is resolved clearly at 1670 cm<sup>-1</sup>, and the  $\nu(\text{CH})$  loss peak is also observed at 2895 cm<sup>-1</sup>. The frequency of  $\nu(\text{CO})$  indicates that the CO double bond is maintained in the molecularly adsorbed formamide.

The decomposition of  $\eta^1(\text{O})\text{-NH}_2\text{CHO}$ <sup>34</sup> is difficult to monitor with EELS, since  $\eta^2(\text{C,O})\text{-NH}_2\text{CO}$  and/or its decomposition products are always present as well, depending on the annealing temperature. Indeed, for a saturation formamide exposure, the  $\eta^2(\text{C,O})\text{-NH}_2\text{CO}$  is stabilized by the higher surface coverage, and a small amount is present to 290 K. As on Ru(001)-p(1×2)-O,<sup>2</sup> the  $\eta^1(\text{O})\text{-NH}_2\text{CHO}$  that is formed undergoes competing desorption and conversion to another surface species at 225 K for a sufficiently high initial exposure (4 L or greater). For formamide exposures between 2 and 4 L, only decomposition of  $\eta^1(\text{O})\text{-NH}_2\text{CHO}$  is observed. This new surface species is stable to approximately 300 K, but it is not easily identifiable due to the presence of several other species on the surface in this temperature range. However, this intermediate does exhibit vibrational loss features at 1675 cm<sup>-1</sup> [ $\nu(\text{CO})$ ] and 2920 cm<sup>-1</sup> [ $\nu(\text{CH})$ ] and lacks the strong  $\omega(\text{NH}_2)$  loss feature at 970 cm<sup>-1</sup> which characterizes  $\eta^2(\text{N,O})\text{-NH}_2\text{CHO}$  on the Ru(001)-p(1×2)-O surface.<sup>2</sup> These vibrational features probably cannot be attributed to  $\eta^1(\text{O})\text{-NH}_2\text{CHO}$ , which, if it does not convert to another species, desorbs well below 300 K. The possible nature of this intermediate, which is identified tentatively as  $\eta^1(\text{N})\text{-NHCHO}$ , will be discussed in Section IV.

Annealing the formamide saturated Ru(001) surface to temperatures in the range of 300 to 350 K causes all of the  $\eta^2(\text{C,O})\text{-NH}_2\text{CO}$  to decompose and all of the ammonia that is formed to desorb, leaving a much simpler EEL spectrum. Identical EEL spectra are obtained if formamide is adsorbed on Ru(001) at room temperature and annealed to 350 K to desorb residual ammonia (cf. Figure 10). (Subsequent exposure to D<sub>2</sub> does not alter these spectra significantly.) The species detected in such EEL spectra include CO, NH, and a small amount of nitrogen adatoms.<sup>31</sup> More significantly, a new surface species is detected which must arise from the decomposition of  $\eta^1(\text{O})\text{-NH}_2\text{CHO}$  via the unidentified intermediate discussed in the previous paragraph. This new species maintains the carbon-hydrogen bond as indicated by a  $\nu(\text{CH})$  loss feature at 2940 cm<sup>-1</sup> and shows a loss feature at 1770

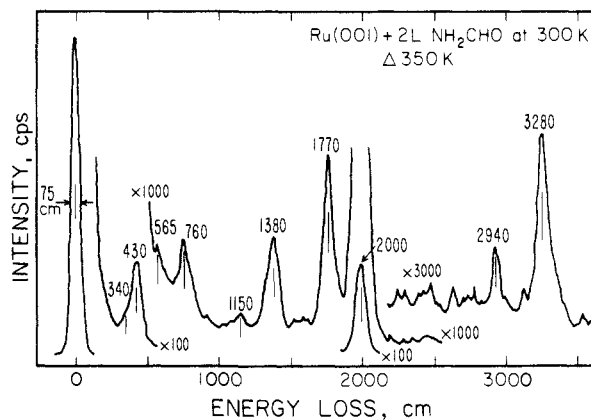


Figure 10. The EEL spectrum that results when the clean Ru(001) surface at 300 K is exposed to 2 L of NH<sub>2</sub>CHO and annealed briefly to 350 K.

cm<sup>-1</sup> that is characteristic of a carbonyl double bond in which the oxygen atom is not coordinated to the metal atom via an electron lone pair donor bond. The new species is thus identified as containing a formyl (HCO) group. Three such species must be considered in determining the identity of this intermediate:  $\eta^1(\text{C})\text{-HCO}$  ( $\eta^1$ -formyl, which could be formed from carbon-nitrogen bond cleavage of formamide),  $\eta^1(\text{N})\text{-NHCHO}$ , and  $\eta^1(\text{N})\text{-NCHO}$ . The possibility of  $\eta^1$ -formyl formation can be ruled out since all  $\eta^1$ -formyl ligands identified in organometallic compounds have a  $\nu(\text{CO})$  frequency between 1540 and 1614 cm<sup>-1</sup>,<sup>35</sup> more than 150 cm<sup>-1</sup> lower than the frequency of 1770 cm<sup>-1</sup> observed in the present case. In addition,  $\eta^1$ -formyl is not observed as a decomposition product of formaldehyde on Ru(001),<sup>10</sup> so its formation from formamide is not expected, especially above 300 K. On the other hand,  $\eta^1(\text{N})\text{-NHCHO}$  ligands identified in organometallic compounds have  $\nu(\text{CO})$  frequencies between 1708 and 1758 cm<sup>-1</sup>,<sup>4</sup> in good agreement with the present data, and an  $\eta^1(\text{N})\text{-NCHO}$  species would be expected to have a similar  $\nu(\text{CO})$  frequency. A definite distinction between  $\eta^1(\text{N})\text{-NHCHO}$  and  $\eta^1(\text{N})\text{-NCHO}$  is not possible because the presence of significant amounts of coadsorbed NH in the EEL spectrum of Figure 10 makes it impossible to determine whether or not the intermediate gives rise to a nitrogen-hydrogen stretching vibration. We tentatively prefer  $\eta^1(\text{N})\text{-NCHO}$  over  $\eta^1(\text{N})\text{-NHCHO}$ , because we believe that the latter species is present below 300 K and would probably undergo NH bond cleavage below 375 K. The identification of this intermediate as  $\eta^1(\text{N})\text{-NCHO}$  would allow all the loss features in Figure 10 to be identified as follows. The intense loss features at 430 and 2000 cm<sup>-1</sup> are due to carbon monoxide, while the features at 3280 and (in part) 1380 cm<sup>-1</sup> are due to NH. The weak feature at 565 cm<sup>-1</sup> indicates that a small amount of NH has decomposed, leaving nitrogen adatoms on the surface. The remaining loss features can be attributed to vibrational modes of  $\eta^1(\text{N})\text{-NCHO}$ :  $\nu(\text{CH})$ , 2940 cm<sup>-1</sup>;  $\nu(\text{CO})$ , 1770 cm<sup>-1</sup>;  $\pi(\text{CH})$ , 1150 cm<sup>-1</sup>;  $\delta(\text{NCO})$ , 760 cm<sup>-1</sup>; and  $\nu_s(\text{RuN})$ , 340 cm<sup>-1</sup>. The peak at 1380 cm<sup>-1</sup> is quite broad and probably derives intensity from  $\delta(\text{CH})$  and  $\nu(\text{CN})$  of  $\eta^1(\text{N})\text{-NCHO}$  as well as from  $\delta(\text{NH})$  of coadsorbed NH, since this peak is more intense [relative to the  $\nu(\text{NH})$  peak] than would be expected if only NH were present. As the surface is annealed to progressively higher temperatures, the loss features at 2940, 1770, 1150, 760, and 340 cm<sup>-1</sup> attenuate and disappear in unison, verifying that they are due to a single surface species. The EEL spectrum of Figure 10 is thus fully consistent with the presence of an  $\eta^1(\text{N})\text{-NCHO}$  species.

Further annealing of the formamide saturated Ru(001) surface

(34) An unknown amount of  $\eta^1(\text{O})\text{-NH}_2\text{CHO}$  also desorbs at 225 K, so that this species undergoes competing desorption and decomposition following exposures  $\geq 4$  L.

(35) (a) Gladysz, J. A.; Tam, W. *J. Am. Chem. Soc.* **1978**, *100*, 2545. (b) Tam, W.; Wong, W.; Gladysz, J. A. *J. Am. Chem. Soc.* **1979**, *101*, 1589. (c) Winter, S. R.; Cornett, G. W.; Thompson, E. A. *J. Organomet. Chem.* **1977**, *133*, 339. (d) Gladysz, J. A.; Williams, G. M.; Tam, W.; Johnson, D. L. *J. Organomet. Chem.* **1977**, *140*, C1. (e) Gladysz, J. A.; Selover, J. C. *Tetrahedron Lett.* **1978**, 319. (f) Collins, T. J.; Roper, W. R. *J. Chem. Soc., Chem. Commun.* **1976**, 1044.

to 375 K causes the  $\eta^1(\text{N})\text{-NCHO}$  to dissociate to carbon monoxide, nitrogen adatoms, and (by inference) hydrogen adatoms, so that only these species and NH remain on the surface. In contrast to the low coverage data, EEL spectra show that some NH is still present on the surface at 400 K, but that it decomposes completely by 430 K. The desorption of CO (and all remaining hydrogen) is complete below 500 K, leaving only nitrogen adatoms on the surface which are manifest in EEL spectra by  $\nu_s(\text{RuN})$  at  $580\text{ cm}^{-1}$ . The recombinative desorption of  $\text{N}_2$  is complete by 810 K, leaving the clean Ru(001) surface following annealing to this temperature.

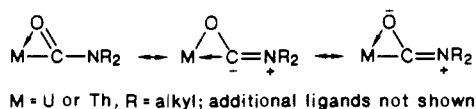
An additional issue of importance is the branching ratio for the two observed decomposition mechanisms of formamide on Ru(001), i.e., of the approximately 0.15 monolayer of formamide that decomposes following a saturation exposure, how much decomposes via  $\eta^2(\text{C,O})\text{-NH}_2\text{CO}$  and how much via  $\eta^1(\text{O})\text{-NH}_2\text{CHO}$  and  $\eta^1(\text{N})\text{-NCHO}$ ? This branching ratio may be estimated by using the intensity of the  $2000\text{-cm}^{-1}$  carbon monoxide loss peak following annealing to 300 K, since by this temperature all the  $\eta^2(\text{C,O})\text{-NH}_2\text{CO}$  has decomposed to CO and either NH or  $\text{NH}_3$ , while little if any of the  $\eta^1(\text{N})\text{-NCHO}$  has yet decomposed. This estimate makes use of the known coverage versus intensity relationship for this CO loss feature.<sup>20</sup> The resulting estimate is that approximately 0.10 monolayer of formamide decomposes via the  $\eta^2(\text{C,O})\text{-NH}_2\text{CO}$  intermediate, while the remaining approximately 0.05 monolayer decomposes via  $\eta^1(\text{N})\text{-NCHO}$ .

Finally, as discussed in Section III.A.1, exposing the clean Ru(001) surface at 80 K to approximately 8 L or more of  $\text{NH}_2\text{CHO}$  results in the condensation of molecular multilayers of formamide, which desorb when the surface is annealed to 210 K. As expected, these multilayers are identical with those formed on the Ru(001)-p(1 $\times$ 2)-O surface.<sup>2b</sup>

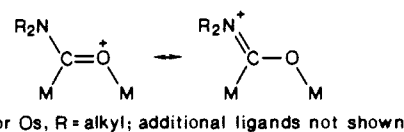
#### IV. Discussion

It has been shown that the adsorption of low coverages of formamide on clean Ru(001) (i.e., where the amount of formamide that decomposes is less than 0.05 monolayer) at 80 K results in CH bond cleavage and rehybridization of the carbonyl double bond to produce an  $\eta^2(\text{C,O})\text{-NH}_2\text{CO}$  species and a hydrogen adatom. No other surface species is identified by EELS below 230 K. The only thermal desorption products detected for these low formamide exposures ( $\leq 2$  L) are CO near 480 K,  $\text{H}_2$  near 420 K,  $\text{N}_2$  near 770 K, and  $\text{NH}_3$  near 315 K. The CO and  $\text{NH}_3$  result from molecular desorption, while the  $\text{H}_2$  and  $\text{N}_2$  result from the recombinative desorption of hydrogen and nitrogen adatoms.

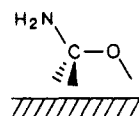
The structure and bonding of the  $\eta^2(\text{C,O})\text{-NH}_2\text{CO}$  is of considerable interest since such a species has not been identified previously on a metal surface. Unfortunately, the lack of a definitive mode assignment due to the presence of significant mode coupling places limits on the conclusions that can be drawn. Several organometallic analogues have been synthesized and characterized, but vibrational data are scarce. In most of these  $\eta^2(\text{C,O})\text{-NR}_2\text{CO}$  ligands, the CO and CN bond orders are less than two and greater than one, so that substantial mode coupling occurs between  $\nu(\text{CO})$  and  $\nu(\text{CN})$ , making the mode descriptions  $\nu_s(\text{NCO})$  and  $\nu_a(\text{NCO})$  more meaningful. A series of mononuclear uranium and thorium compounds have been synthesized with the metal-formide group represented by the resonance structures shown below.<sup>5a</sup>



These compounds have  $\nu_s(\text{NCO})$  frequencies between  $1491$  and  $1559\text{ cm}^{-1}$  and  $\nu_a(\text{NCO})$  frequencies between  $1298$  and  $1346\text{ cm}^{-1}$ . Also relevant to  $\eta^2(\text{C,O})\text{-NH}_2\text{CO}$  on Ru(001) are the  $\eta^2(\text{C,O})\text{-NR}_2\text{CO}$  ligands in several trinuclear ruthenium<sup>5c,e</sup> and osmium<sup>5b,d</sup> complexes, the structures of which have been represented as follows:



Although IR data with mode assignments are not available for these compounds, X-ray structures show clearly that both the CO and CN bonds of the OCN group have bond lengths intermediate between those expected for single and double bonds. For example, the  $\text{OCN}(\text{CH}_3)_2$  ligand in  $\text{HRu}_3(\text{OCN}(\text{CH}_3)_2)(\text{CO})_{10}$  has CO and CN bond lengths of  $1.287$  and  $1.340\text{ \AA}$ ,<sup>5c</sup> respectively, while "typical" C=O, C—O, C=N, and C—N bond lengths are approximately  $1.22$ ,  $1.43$ ,  $1.27$ , and  $1.47\text{ \AA}$ , respectively.<sup>36</sup> We expect that the structure of  $\eta^2(\text{C,O})\text{-NH}_2\text{CO}$  on Ru(001) is similar to the structures observed for the  $\eta^2(\text{C,O})\text{-NR}_2\text{CO}$  ligands in these trinuclear ruthenium and osmium complexes, and indeed the rehybridization of the CO bond may occur to an even greater extent on the extended ruthenium surface due to the following additional resonance structure:



The species most closely related to  $\eta^2(\text{C,O})\text{-NH}_2\text{CO}$  that has been identified previously on Ru(001) is  $\eta^2(\text{C,O})\text{-HCO}$  ( $\eta^2$ -formyl), which is formed (along with chemisorbed CO and hydrogen adatoms) following relatively low exposures of formaldehyde to this surface at 80 K.<sup>10</sup> The  $\eta^2$ -formyl has a  $\nu(\text{CO})$  frequency of  $1180\text{ cm}^{-1}$ , indicative of a CO bond order of approximately 1.3. In this case, the assignment of  $\nu(\text{CO})$  is straightforward and meaningful, because coupling to the CH bending modes is insignificant. (The mode identified as  $\nu(\text{CO})$  shifts down only slightly to  $1160\text{ cm}^{-1}$  upon deuteration of the formyl.) The decomposition of  $\eta^2(\text{C,O})\text{-NH}_2\text{CO}$  is similar to that of  $\eta^2$ -formyl on Ru(001) in that carbon monoxide is the only oxygen- or carbon-containing decomposition product. The  $\eta^2(\text{C,O})\text{-NH}_2\text{CO}$  is considerably more stable than  $\eta^2$ -formyl, however, since the latter decomposes to carbon monoxide and hydrogen adatoms upon annealing to only 120 K. The fact that formamide can undergo CH bond cleavage at 80 K on Ru(001) is not surprising in view of the fact that formaldehyde does. The CH bond energies of these two molecules are similarly low:  $87\text{ kcal}$  in formaldehyde<sup>37</sup> and  $89\text{ kcal}$  in formamide.<sup>38</sup>

The spectroscopically observed decomposition products of  $\eta^2(\text{C,O})\text{-NH}_2\text{CO}$ , appearing in the temperature range  $230\text{--}250\text{ K}$ , are CO,  $\text{NH}_3$ , and NH. Additional hydrogen adatoms also result from the decomposition of this species, since very little ammonia ( $\leq 0.02$  monolayer) is produced. The rate-limiting step in this decomposition is almost certainly CN bond cleavage to produce  $\text{NH}_2$  and CO, because if NH bond cleavage preceded CN bond cleavage,  $\text{NH}_3$  would probably not be formed.<sup>39</sup> Since  $\text{NH}_2$  is not observed spectroscopically, it is concluded that this species is unstable on Ru(001) at 250 K (on the time scale of seconds at these surface coverages) and rapidly dehydrogenates to NH or is hydrogenated by a hydrogen adatom to  $\text{NH}_3$ . The ammonia that is produced desorbs molecularly at 315 K, in agreement with previous studies of ammonia adsorption on Ru(001).<sup>14a</sup>

The NH species observed on Ru(001) from formamide decomposition is only the second NH species that has been identified spectroscopically on a metal surface. The first was NH formed from hydrazine decomposition on Ni(111),<sup>32</sup> and Table IV shows

(36) The "typical" bond lengths are estimated from covalent radii. See: Jolly, W. L. *The Principles of Inorganic Chemistry*; McGraw-Hill: New York, 1976; p 36.

(37) Golden, D. M.; Benson, S. W. *Chem. Rev.* **1969**, *69*, 125.

(38) Kahumoto, T.; Saito, K.; Imamura, A. *J. Phys. Chem.* **1985**, *89*, 2286.

(39) Preliminary experiments with coadsorbed NH and hydrogen and coadsorbed ammonia and hydrogen suggest that NH cannot be hydrogenated to ammonia on Ru(001) under UHV conditions, and also that deuterium adatoms do not exchange into adsorbed ammonia. Parmeter, J. E., unpublished results.



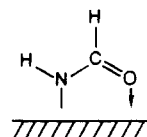
that the vibrational frequencies of the two species are quite similar. Since the only examples known to us of NH ligands in organometallic complexes are in complexes containing at least three metal atoms with the nitrogen atom in a threefold hollow site among three metal atoms,<sup>40</sup> it is very likely that NH on Ru(001) occupies threefold hollow sites as well. This is undoubtedly also true of the NH on Ni(111), a surface that has the same hexagonally close-packed structure as Ru(001).

The decomposition of ND<sub>2</sub>CHO on Ru(001) leads to the formation of chemisorbed ammonia, with ND<sub>2</sub>H and ND<sub>3</sub> being formed in an approximate ratio of 3:2. We suspect that the minor amounts of NDH<sub>2</sub> and NH<sub>3</sub> that are formed result from sample contamination by NHDCHO and NH<sub>2</sub>CHO. The adsorption at 80 K of pure ND<sub>2</sub>CHO would produce  $\eta^2(\text{C,O})\text{-ND}_2\text{CO}$  and hydrogen adatoms. Decomposition of  $\eta^2(\text{C,O})\text{-ND}_2\text{CO}$  would then produce (presumably) a short-lived ND<sub>2</sub> species, which would either dehydrogenate to ND with the production of a deuterium adatom or be hydrogenated to ammonia by a hydrogen adatom or, in some cases, by a deuterium adatom formed from ND<sub>2</sub> decomposition to ND. Since there will be more hydrogen adatoms present on the surface than deuterium adatoms, the ammonia that is formed would be mainly ND<sub>2</sub>H with a smaller amount of ND<sub>3</sub>. The formation of some NDH<sub>2</sub> could conceivably result from H/D exchange into ND<sub>2</sub>H, but preliminary results suggest that this reaction should not occur under these conditions.<sup>39</sup> As expected, the "NH" formed from ND<sub>2</sub>CHO decomposition is almost entirely ND, and the small amount of NH formed may result from sample contamination or from H exchange into ND.

For sufficiently high formamide exposures ( $\geq 2$  L) to the Ru(001) surface at 80 K, molecularly adsorbed  $\eta^1(\text{O})\text{-NH}_2\text{CHO}$  is observed in EELS in addition to  $\eta^2(\text{C,O})\text{-NH}_2\text{CO}$ . This indicates that the initial products of adsorption,  $\eta^2(\text{C,O})\text{-NH}_2\text{CO}$  and hydrogen adatoms, passivate the surface with respect to subsequent CH bond cleavage and CO bond rehybridization so that at higher coverages the molecularly adsorbed  $\eta^1(\text{O})\text{-NH}_2\text{CHO}$  species is formed as on the Ru(001)-p(1 $\times$ 2)-O surface.<sup>2</sup> A similar but more complex situation occurs in the case of formaldehyde adsorption on Ru(001), where the following adsorption products appear sequentially with increasing exposure at 80 K: CO + 2H,  $\eta^2(\text{C,O})\text{-HCO}$  + H,  $\eta^2(\text{CO})\text{-H}_2\text{CO}$ , and  $\eta^1(\text{O})\text{-H}_2\text{CO}$ .<sup>10</sup> In the case of formamide adsorption on Ru(001) at 80 K, no  $\eta^2(\text{C,O})\text{-NH}_2\text{CHO}$  species is detected unambiguously for intermediate formamide exposures, which might have been expected from the formaldehyde results. It is possible, however, that such a species is formed in small amounts, but that its loss features cannot be resolved from those of the other surface species that are present.

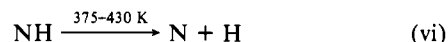
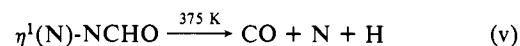
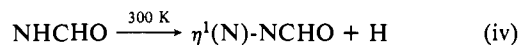
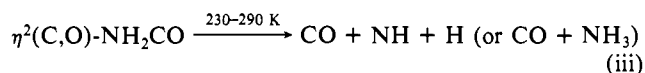
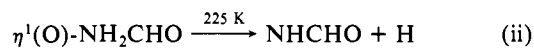
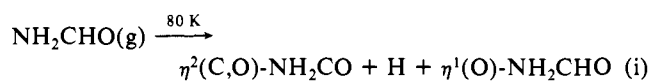
The  $\eta^1(\text{O})\text{-NH}_2\text{CHO}$  decomposes completely upon annealing for formamide exposures less than 4 L (amount of formamide decomposing less than approximately 0.10 monolayer), whereas for exposures greater than 4 L it undergoes competing desorption and decomposition at 225 K. While we have no quantitative estimate of the amount of  $\eta^1(\text{O})\text{-NH}_2\text{CHO}$  that desorbs molecularly, the amount that decomposes following a saturation formamide exposure is approximately 0.05 monolayer. Two stable decomposition intermediates are observed in the decomposition of  $\eta^1(\text{O})\text{-NH}_2\text{CHO}$ , one that is present from approximately 225 to 300 K and the second from 300 to 375 K. The species that is stable from approximately 300 to 375 K is probably  $\eta^1(\text{N})\text{-NCHO}$ , analogous to the NH species formed from  $\eta^2(\text{C,O})\text{-NH}_2\text{CO}$  decomposition, but with the hydrogen atom replaced by a formyl group. This species decomposes to CO, nitrogen adatoms, and hydrogen adatoms upon annealing the surface to 375 K. The first intermediate, present from 225 to 300 K, contains a carbon-oxygen double bond [ $\nu(\text{CO}) = 1675 \text{ cm}^{-1}$ ] and a carbon-hydrogen bond [ $\nu(\text{CH}) = 2920 \text{ cm}^{-1}$ ], but it lacks the intense  $\omega(\text{NH}_2)$  loss feature at  $970 \text{ cm}^{-1}$  that characterizes  $\eta^2(\text{N,O})\text{-NH}_2\text{CHO}$  on Ru(001)-p(1 $\times$ 2)-O,<sup>2</sup> a species that is formed on that surface by conversion of  $\eta^1(\text{O})\text{-NH}_2\text{CHO}$  at 225 K and which is bonded to the surface via electron lone pairs on both the oxygen

and nitrogen atoms. While the identification of this intermediate is uncertain, it seems likely that the coordination of the nitrogen atom to the surface must occur at 225 K in order to lead to the eventual formation of  $\eta^1(\text{N})\text{-NCHO}$ . We suggest that on Ru(001) this occurs via nitrogen-hydrogen bond cleavage to produce an N-bonded NHCHO species that maintains the carbonyl double bond and the donor bond between the oxygen atom and the metal surface, as shown below:



This species could convert to  $\eta^1(\text{N})\text{-NCHO}$  at 300 K by simultaneously undergoing cleavage of the remaining nitrogen-hydrogen bond and the oxygen-ruthenium donor bond. It is not clear in detail, however, why such an N-bonded NHCHO species would not convert to the formate-like species  $\eta^2(\text{N,O})\text{-NHCHO}$  [cf. Figure 1, species 4], which is formed upon nitrogen-hydrogen bond cleavage of  $\eta^2(\text{N,O})\text{-NH}_2\text{CHO}$  at 265 K on Ru(001)-p(1 $\times$ 2)-O.<sup>2</sup> In general, the answer undoubtedly lies largely in the differing electronic properties of the Ru(001) and Ru(001)-p(1 $\times$ 2)-O surfaces.

A final issue to be addressed is the complex nature of the hydrogen thermal desorption spectra. For a saturation formamide exposure, the following reactions produce hydrogen adatoms as the surface is heated [assuming the presence of both N-bonded NHCHO and NCHO intermediates in  $\eta^1(\text{O})\text{-NH}_2\text{CHO}$  decomposition]:



Here (g) denotes a gas-phase species, and all other species are adsorbed. If we consider a saturation exposure of ND<sub>2</sub>CHO and neglect contamination by NHDCHO or NH<sub>2</sub>CHO, reactions i and v will produce hydrogen adatoms, while reactions ii, iii, iv, and vi will produce deuterium adatoms.<sup>41</sup> Although the four hydrogen desorption peaks at 280, 300, 375, and 410 K (cf. Figure 4) cannot be assigned exclusively to surface hydrogen produced by any single reaction listed above, several conclusions can be drawn. First, since NH decomposes above 375 K, the hydrogen produced by NH decomposition must desorb in the 410 K peak (with perhaps a small amount desorbing in the 375 K peak). Indeed, the desorption of hydrogen at 300 K is a minor piece of evidence supporting the decomposition of  $\eta^1(\text{N})\text{-NHCHO}$  to  $\eta^1(\text{N})\text{-NCHO}$  at this temperature. This scheme is also in agreement with thermal desorption results for ND<sub>2</sub>CHO that show the 410 K peak to contain mainly D<sub>2</sub>, a result that shows the hydrogen in this peak is derived largely from the ND<sub>2</sub> group of the initially adsorbed formamide. Some HD also desorbs at 410 K since not all of the hydrogen adatoms formed by reaction v desorb immediately in the 375 K peak. Thus, while not all hydrogen in the 410 K peak results from NH decomposition, it is NH decomposition near 410 K that increases the surface hydrogen (H or D) adatom concentration and serves to trigger this intense

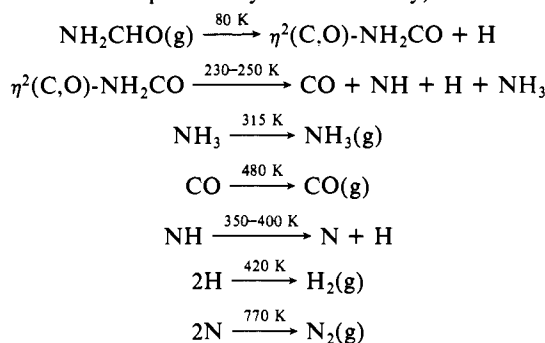
(40) (a) Fjare, D. E.; Gladfelter, W. L. *J. Am. Chem. Soc.* **1981**, *103*, 1572. (b) Fjare, D. E.; Gladfelter, W. L. *Inorg. Chem.* **1981**, *20*, 3533.

(41) This analysis also assumes that no H/D exchange occurs among the various adsorbed surface species.

desorption peak. Similarly, the desorption of hydrogen at 280, 300, and 375 K is probably triggered by reactions iii, iv, and v, respectively.<sup>42</sup> Indeed, the desorption of hydrogen at 300 K is a minor piece of evidence supporting the decomposition of  $\eta^1$ (N)-NHCHO to  $\eta^1$ (N)-NCHO at this temperature. This scheme is also consistent with large amounts of HD in the 375 K peak (cf. Section III.A.3), since reaction v produces hydrogen adatoms that will recombine with adatoms on the surface, and the latter will be primarily deuterium rather than hydrogen. We emphasize once again that the problem of sample contamination (and, to a lesser degree, the difficulty of peak deconvolution) makes a more quantitative analysis of the amounts of H<sub>2</sub>, HD, and D<sub>2</sub> desorbed in each peak impossible.

## V. Conclusions

Following a saturation formamide exposure on the clean Ru(001) surface at 80 K, approximately 0.15 monolayer of formamide decomposes. This decomposition occurs via two distinct mechanisms. The major one, accounting for 0.10 monolayer of formamide that decomposes at saturation, is the only decomposition mechanism that occurs at low coverage and may be written as follows (the temperatures given are for the low coverage limit, and the second step is clearly not elementary):



(42) The fact that an H<sub>2</sub> thermal desorption peak occurs at 300 K following saturation exposures supports the idea of a dehydrogenation reaction occurring at this temperature and thus, indirectly, supports the presence of an N-bonded NHCHO species which converts to an N-bonded NCHO species.

(43) Suzuki, I. *Bull. Chem. Soc. Jpn.* **1960**, *33*, 1359.

(44) (a) Evans, J. C. J. *Chem. Phys.* **1954**, *22*, 1228. (b) King, S. T. J. *Phys. Chem.* **1971**, *75*, 405.

**Table IV.** Vibrational Frequencies (cm<sup>-1</sup>) and Mode Assignments for NH and ND on Ru(001) (This Work) and Ni(111)<sup>32</sup>

mode	Ru(001)			Ni(111)		
	NH	ND	Shift	NH	ND	Shift
$\nu(\text{NH})$	3315	2460	1.35	3340	2480	1.35
$\delta(\text{NH})$	1350	1050	1.29	1270	950	1.34
$\nu(\text{M-NH})$	690	680	1.01	620	580	1.07

At saturation, approximately 0.08 monolayer of NH and 0.02 monolayer of NH<sub>3</sub> are produced.

For exposures greater than 2 L, where the amount of formamide that decomposes is greater than approximately 0.05 monolayer, a second decomposition mechanism occurs. In this mechanism,  $\eta^1$ (O)-bonded molecular formamide, formed from formamide adsorption at 80 K, converts near 225 K to an intermediate believed to be an N-bonded NHCHO species. At 300 K, this intermediate converts to an intermediate tentatively identified as  $\eta^1$ (N)-NCHO, a species analogous to NH but with the hydrogen atom replaced by a formyl group. This intermediate decomposes near 375 K to coadsorbed carbon monoxide, and nitrogen and hydrogen adatoms. For exposures greater than 4 L, where the amount of formamide that decomposes is greater than approximately 0.09 monolayer, some molecular desorption of  $\eta^1$ (O)-NH<sub>2</sub>CHO occurs also at 225 K.

The reactions and surface intermediates observed in formamide decomposition on clean Ru(001) and on Ru(001)-p(1×2)-O are quite different. However,  $\eta^1$ (O)-NH<sub>2</sub>CHO is formed on both surfaces under certain conditions of coverage and temperature. The amount of formamide that decomposes following a saturation exposure increases by a factor of 3, from 0.05 to 0.15 monolayer, in going from the oxygen covered to the clean surface.

**Acknowledgment.** The authors are grateful to Dr. Malina Hills for assistance in obtaining the ammonia thermal desorption spectra. This research was supported by the National Science Foundation (Grant No. CHE-8516615) and the donors of the Petroleum Research Fund, administered by the American Chemical Society.

**Registry No.** NH<sub>2</sub>CHO, 75-12-7; Ru, 7440-18-8; NH<sub>3</sub>, 7664-41-7; CO, 630-08-0.

## Resonance Raman Spectroscopic Study of Bilirubin Hydrogen Bonding in Solutions and in the Albumin Complex

You-Zung Hsieh and Michael D. Morris\*

Contribution from the Department of Chemistry, University of Michigan, Ann Arbor, Michigan 48109. Received May 20, 1987

**Abstract:** Resonance Raman spectra are reported for bilirubin in chloroform, dimethyl sulfoxide, and aqueous solutions, and for the 1:1 bilirubin/albumin complex and the bilirubin complexes of  $\alpha$ - and  $\beta$ -cyclodextrin. From the known hydrogen-bonding patterns in the several free solutions, Raman markers for the presence or absence of internal hydrogen bonding are derived. From equilibrium and time-resolved deuteration, partial assignments of the spectra are proposed. The resonance Raman spectrum of the bilirubin/albumin complex demonstrates that the internal hydrogen bonds between propionate groups and the pyrrro-methenone rings are ruptured. Propionate hydrogen bonding is to amino acid residues of the protein only.

(4Z,15Z)-Bilirubin IX $\alpha$  (structure **1a**), commonly called bilirubin, is the final product of hemoglobin metabolism.<sup>1</sup> The molecule is only sparingly soluble in aqueous solutions, although

the dipropionate anion (structure **1b**) is soluble in alkaline solution. Bilirubin is carried through the bloodstream to the liver as an albumin complex. In the liver the water-soluble glucuronic acid ester is formed. Bilirubin diglucuronide is then transported to the kidneys and excreted in the urine.

Historically, bilirubin has been considered as merely a toxic waste product<sup>2</sup> with an interesting chemistry. If bilirubin is not

(1) (a) Heirweigh, K. P. M.; Brown, S. B., Eds. *Bilirubin*; CRC Press: Boca Raton, FL, 1982; Vol. 1. (b) McDonagh, A. F. In *The Porphyrins*; Dolphin, D., Ed.; Academic Press: New York, 1979; Vol. 6, pp 293-491.